THE JOURNAL OF PHYSICAL CHEMISTRY B

ARTICLE

pubs.acs.org/JPCB

Insights into the Mechanism of Aggregation and Fibril Formation from Bovine Serum Albumin

Mily Bhattacharya, Neha Jain, and Samrat Mukhopadhyay*

Indian Institute of Science Education and Research (IISER) Mohali, Sector 81, S.A.S Nagar, Mohali 140306, India

Supporting Information

ABSTRACT: We have investigated the fibrillation propensity of different conformational isomers of an archetypal, all α-helical protein, namely, bovine serum albumin (BSA), under different pH conditions and ionic strengths using fluorescence and circular dichroism (CD) spectroscopy. At low pH and higher protein concentration, the partially folded conformers associate to form oligomers that are converted into ordered amyloid-like fibrils when incubated at elevated temperature. We have elucidated the mechanism of fibril formation, especially the early steps, by monitoring the kinetics of structural changes during the aggregation process. Various structural probes in tandem were utilized to decipher the temporal evolution of both conformational and size changes by measuring the time dependence of fluorescence intensity and anisotropy of intrinsic tryptophans and several extrinsic fluorophores during the aggregation. Additionally, CD spectroscopy was utilized to monitor the changes in protein secondary structural content during fibrillation. Our findings suggest that the conformational conversion occurs in the oligomers that serve as precursors to amyloid fibrils and precedes the overall fibrillar growth.

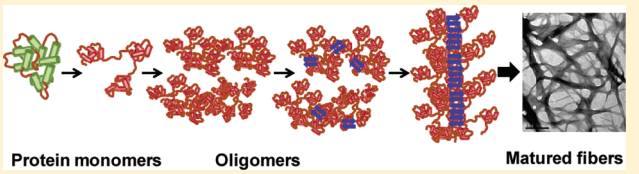

1. INTRODUCTION

Protein misfolding leading to amyloid aggregation has been implicated in a whole range of debilitating neurodegenerative disorders.[1−8] The diseases are characterized by deposition of insoluble plaques consisting of β-sheet-rich amyloid fibrils. The fact that many proteins, irrespective of their native structures, can form nonpathogenic β-sheet-rich amyloid fibrils under carefully designed in vitro conditions has led to the consensus that amyloid formation is a generic property of the polypeptides.[9−11] The key step in the amyloid fibril formation involves destabilization of protein's native conformation, induced by a change in pH, temperature, and ionic strength, etc., which results in the formation of partially folded intermediates.[12−15] These conditions promote the accumulation of a significant population of partially folded conformers which are otherwise inaccessible under normal conditions. Such nonnative intermediates can undergo conformational rearrangements mediated by reorganization of specific noncovalent intermolecular interactions, e.g., hydrogen bonding, electrostatic interactions, hydrophobic contacts that subsequently lead to oligomerization and fibril formation. The fibril organization and assembly, fibrillation kinetics, and the overall stability of the fibrils are significantly influenced by the amino acid sequence and the environmental conditions.[16,17] In addition to accumulation of amyloid fibrils which is detrimental to normal well-being, oligomeric intermediates are proposed to be more harmful than the fibrils themselves as they have been shown to permeabilize cell membranes of living cells.[18−20] Hence, an in-depth comprehension of the underlying principles of oligomerization followed by fibril formation is very crucial in addition to the various studies aimed at inhibition of amyloidosis.[21,22]

The seminal observation that an all α-helical protein can form β-rich amyloid-like aggregates, despite having no predisposition toward β-sheet formation, has spurred a lot of interest in recent years.[11] An interesting question in this area is how an all α-helical protein transforms into β-rich conformation, in response to modification of solution conditions, e.g., pH, ionic strength, and temperature favoring a partially destabilized state, that ultimately culminates in amyloid fibril formation. We have used serum albumin as a model all α-helical protein for the present study. Serum albumin is a globular, all α-helical protein present in the circulatory system which is the most abundant of all plasma proteins (∼60%) with an average concentration of 50 g/L. It is primarily a carrier protein that is involved in the binding and transport of fatty acids, hormones, metabolites, endogenous ligands, and drug delivery in addition to the maintenance of colloid osmotic blood pressure.[23,24] It has been demonstrated that serum albumin is majorly responsible for the preservation of blood pH as changes in the plasma protein concentration can induce either acidosis or alkalosis that results in albumin-related diseases.[25] Human serum albumin (HSA) or its bovine analogue (BSA) is a 585-residue, multidomain, all-α-helical protein that adapts a heart-shaped structure at physiological pH (Figure 1). The crystal structure of HSA[26,27] shows that each of the three homologous domains (I, II, and III) is further composed of two

Received: December 3, 2010
Revised: February 25, 2011
Published: March 21, 2011

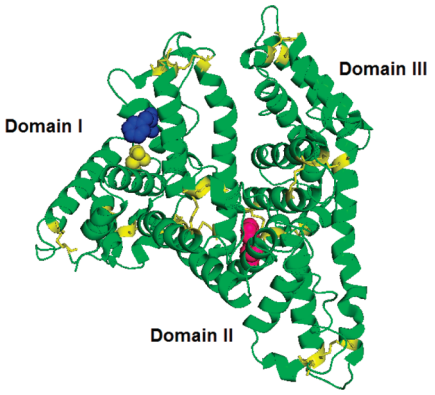

Figure 1. Crystal structure of HSA showing the cysteine (C34; yellow sphere), single tryptophan (W214; magenta sphere), phenylalanine (F134; blue sphere), and disulfides (yellow sticks) generated using PyMol (DeLano Scientific LLC, CA, USA) from protein data bank (1UOR). BSA shares 76% sequence homology with HSA. BSA contains one more tryptophan in domain I at position 134 instead of the phenylalanine.

subdomains (A and B) that contain several intradomain disulfide bonds (17 disulfide bridges in total) which impart rigidity to the helical, globular structure but allow enough flexibility to the protein to undergo conformational changes in response to changes in pH[28] and upon interaction with fatty acids.[23] BSA shares a 76% sequence homology with HSA, contains one more tryptophan residue in domain I (in addition to the one in domain II), and also undergoes reversible conformational isomerization as a function of pH.[29,30] The physiological relevance of serum albumins might be linked to pH-dependent binding and release of substrates given the fact that low pH has been measured on the membrane surfaces of several tissues.[31]

Various studies have been directed toward the design of optimum conditions and probing the mechanistic aspects of both human and bovine serum albumin aggregation.[32−39] However, the time course of the structural transition from the partially unfolded monomeric conformer to the fibrillar state still remains elusive despite the fact that different morphologies of serum albumin aggregates have been characterized in the earlier studies. Additionally, the early key events in the aggregation of serum albumin are yet to be elucidated. Also, limited attempts have been made to examine BSA aggregation at low pH[36] though, as mentioned earlier, a low-pH regime is also important in the physiological context as the region near membrane surfaces of a few tissues is acidic. Very recently, it has also been reported that BSA forms "globular amyloid-like aggregates" upon glycation with D-ribose (which induces conformational changes in native BSA) that exhibit high cytotoxicity toward neuronal cell lines by increasing the intracellular level of reactive oxygen species (ROS).[40] Therefore, combining all the facts stated above given with the primary role of serum albumin as carrier proteins, it is important to investigate the aggregation mechanism of serum albumin at other solution conditions, especially at low pH, and delineate the earliest steps that eventually drive the aggregation process forward, and this is expected to illuminate the molecular mechanism of serum albumin aggregation.

In this work, we have carried out a systematic study on the structural changes of BSA under several pH conditions in the aggregated state. Detailed information on conformational changes associated with the overall size variation during aggregation were extracted by using steady-state fluorescence spectroscopy. Fluorescence spectroscopy has proved to be a useful and powerful methodology to extract information about the structural and mechanistic characterization of amyloid fibrils.[41−45] The uniqueness of fluorescence spectroscopy lies in the fact that the conformational changes occurring simultaneously with size changes can be detected, which is important for gaining insights into the mechanistic pathway of amyloidosis. Additionally, the secondary structural changes in the conformational isomers were monitored by circular dichroism (CD) spectroscopy. In the present study, we have been able to decipher the early key steps in the fibrillation event by monitoring the kinetics of both conformation and size change simultaneously. Multiple structural probes were utilized in tandem to unravel the key steps involved in the aggregation, and a plausible molecular mechanism of serum albumin aggregation has been suggested on the basis of our experimental observations and existing models.

2. EXPERIMENTAL METHODS

2.1. Materials. Bovine serum albumin (fatty acid depleted, catalog no. A7906), glycine, sodium phosphate monobasic, sodium phosphate dibasic, sodium chloride, and potassium chloride were purchased from Sigma (St. Louis, MO) and used without any further purification. The fluorescent probes, viz., 8-anilinonaphthalene,1-sulfonic acid ammonium salt (ANS), and thioflavin-T (ThT), were obtained from Sigma and 5-((((2-iodoacetyl)amino)ethyl)amino)naphthalene-1-sulfonic acid (IAEDANS) was procured from Molecular Probes, Invitrogen Inc., and used as received. Milli-Q water was used for preparation of solutions and buffers. KCl−HCl (pH 1.6, 2), glycine−HCl (pH 2.5, 3), sodium citrate (pH 3.5−6), sodium phosphate mono- and dibasic (pH 6.5−8), Tris-HCl (pH 8.5), and glycine−NaOH (pH 9−10.5) were used for buffer preparations. All buffers (from pH 1.6 to pH 10.5) were prepared freshly and adjusted by adding 1 N HCl or NaOH prior to every pH titration and aggregation experiment. The pH of the buffers was checked on a Cyberscan pH 510 bench meter from Eutech Instruments. The final pH was in the range of ±0.01 at 24−25 °C.

2.2. Preparation of Protein Sample for Aggregation. BSA was dissolved in 5 mM phosphate buffer of pH 7 to give a stock solution of 1 mM and stored at 4 °C. Accurate protein concentration was determined by measuring the absorbance of tryptophans at 280 nm on Lambda 25, Perkin-Elmer UV−visible spectrophotometer. The molar extinction coefficient of BSA at 280 nm is 43 824 M^{-1} cm^{-1}.[24] In a typical aggregation experiment, 1 mM of BSA (5 mM phosphate, pH 7) was diluted 10-fold using a buffer (pH 3, 50 mM Gly−HCl) to yield a final protein concentration of 100 μM (~6 mg/mL) at pH 3. The protein samples were incubated with a desired concentration of NaCl and heated to 65 ± 1 °C in a heating block preset at the required temperature without agitation. For aggregation studies using labeled BSA, a mixture of unlabeled and labeled protein was prepared so that the labeled protein content was 5% of the total protein concentration.

2.3. Fluorescence Labeling of BSA. The labeling of the thiol group of cysteine was carried out in 50 mM, phosphate buffer of pH 7.4. Approximately, 10 equiv of IAEDANS, dissolved in dry dimethyl sulfoxide (DMSO), was added to BSA solution in phosphate buffer of pH 7.4, and the reaction mixture was kept in the dark for overnight under quiescent condition. After the labeling reaction was complete, the labeled protein was purified

in two stages. In the first step, the labeled protein was passed through a desalting column whereby the free, unreacted dye was removed. To ensure complete removal of noncovalently bound IAEDANS from BSA, the labeled protein was again purified and concentrated using a Microcon centrifugal filter (30 kDa cutoff; obtained from Millipore). The concentrated protein was diluted in a phosphate buffer (50 mM, pH 7.4), and the concentration was checked by measuring the absorbance at both 280 (tryptophan) and 337 nm (AEDANS). The concentration of the labeled protein was determined by subtracting the absorption contribution of AEDANS at 280 nm. The molar extinction coefficient of IAEDANS at 280 and 337 nm is 1060 [46] and 6100 M^{-1} cm^{-1},[47] respectively. The AEDANS fluorescence was measured at 475 nm (excitation wavelength 375 nm).

2.4. Fluorescence Measurements. All of the steady-state fluorescence measurements were performed on an LS 55 luminescence spectrometer from Perkin-Elmer at room temperature (~24 °C). For monitoring the tryptophan fluorescence, aliquots of the protein sample (100 μM) were taken out at regular intervals, diluted 10-fold using a buffer (50 mM, phosphate, pH 7.4), and allowed to cool at room temperature prior to fluorescence measurements. For ANS fluorescence-based aggregation experiments, ANS concentration of 10 μM was used which was obtained by suitable dilution of a stock solution (10 mM) of ANS (prepared in Milli-Q water and stored at 4 °C) into protein solution prior to the heating required for aggregation. Aliquots from the aggregate sample were withdrawn at regular intervals and allowed to cool at room temperature, and the fluorescence properties of ANS were measured without any further dilution. For aggregation studies using labeled BSA, aliquots from the labeled sample mixture were cooled at ~24 °C and used without any further dilution for measuring the fluorescence intensity and anisotropy. For all of the experiments, the fluorescence intensity and anisotropy were collected at constant wavelength with an integration time of 5 and 30 s, respectively. The steady-state anisotropy is given by $r = (I_{II} - GI_{\perp})/(I_{II} + 2GI_{\perp})$, where I_{II}, $I_{\perp}$ are fluorescence intensities collected using parallel and perpendicular geometry of the polarizers, respectively, and the perpendicular components were corrected using respective G-factors. The error associated with the fluorescence anisotropy measurements was below 0.01. All of the emission spectra were scanned at a rate of 10 nm/min and averaged over five scans. The following parameters were adjusted for monitoring tryptophan fluorescence intensity and anisotropy during aggregation experiments: λ_{ex} = 300 nm, λ_{em} = 350 nm, excitation bandpass = 2.5 nm, and emission bandpass = 4 (for intensity) and 7−9 nm (for anisotropy). For recording ANS fluorescence intensity and anisotropy, the following parameters were used: λ_{ex} = 350 nm, λ_{em} = 475 nm, and emission bandpass = 4 (for intensity) and 6 nm (for anisotropy). For monitoring AEDANS fluorescence anisotropy, these were the parameters: λ_{ex} = 375 nm, λ_{em} = 475 nm, excitation bandpass = 2.5 nm, and emission bandpass = 6−7 nm. Several data points at a given condition were collected to get an estimate of the standard deviation associated with the measurement. The graphs were plotted using commercially available OriginPro Version 8.0 software and, wherever required, fitted using nonlinear least-squares curve fitting. The goodness of the fit was determined by the adjusted R^2 value (which was typically in the range of 0.97−0.99) and the respective residual plots.

2.5. Thioflavin-T Fluorescence Assay. Thioflavin-T (ThT) fluorescence was measured to monitor amyloid aggregation of BSA (unlabeled) as a function of time. Typically, 50 μL of protein aggregate sample in Gly−HCl buffer (50 mM, pH 3) was diluted 10-fold by using a phosphate buffer (50 mM, pH 7.4) containing ThT to a final concentration of 18 μM ThT in pH 7.4 at room temperature. The following parameters were adjusted for monitoring ThT fluorescence intensity during aggregation experiments: λ_{ex} = 450 nm, λ_{em} = 480 nm, excitation bandpass = 2.5 nm, and emission bandpass = 5 nm.

2.6. Circular Dichroism Spectroscopy. The far-UV CD spectra of the protein samples were recorded on a J-810 Jasco CD spectrometer at room temperature. Typically, the protein sample solution at a given pH was diluted 30-fold to a final protein concentration of 3 μM, which was taken in a quartz cuvette of 1 mm path length, and the secondary structural changes were recorded in the range of 195−250 nm. The scan rate was 100 nm/min, and the final spectrum was averaged over five scans. The spectra were corrected with buffer baseline subtraction.

2.7. Transmission Electron Microscopy. The sample was transferred onto a carbon-coated copper grid and dried in air for 2−3 h and then under vacuum for 5 h. It was then stained with 0.2% aqueous uranyl acetate solution and dried under vacuum for 5 h. The transmission electron microscopy (TEM) images were recorded on an FEI Tecnai T20 microscope at an operating voltage of 200 kV.

3. RESULTS

Prior to embarking on our aggregation studies, we investigated the conformational and size changes of monomeric BSA by fluorescence and CD spectroscopy as a function of pH.[48] The fluorescence intensity of a fluorophore is sensitive to its environment, which suggests that changes observed in the intrinsic tryptophan fluorescence intensity can be correlated to the protein conformational changes.[49] The fluorescence anisotropy measurements provide information about the overall size and the rigidity of the probe attached to biomolecules. The steady-state fluorescence anisotropy is related to the overall size of the protein assuming that the overall size change is predominant compared to the changes in internal (local) dynamics. This assumption is supported by a concentration-dependent increase in the fluorescence anisotropy of various intrinsic and extrinsic labels (Figure S3 in Supporting Information). Recently, we have reported that at low protein concentration where BSA is predominantly monomeric, population of a few but distinct conformational isomers in the acidic, neutral, and alkaline pH range could be clearly identified and characterized using a variety of fluorescence observables.[48] The conformational isomers, especially in the acidic pH, showed a decrease in helical content with an increase in the hydrophobicity which indicated the existence of "molten-globule-like" expanded conformers and were expected to be amyloidogenic precursors. These findings set the stage for further investigations into the structural and mechanistic aspects of the aggregation process at higher protein concentrations.

3.1. Aggregation of BSA. The aggregation and fibrillation propensity of different conformational isomers of BSA at different pH in the presence of salt was investigated by changes in the thioflavin-T (ThT) fluorescence intensity. ThT is an amyloid reporter which when bound to amyloid fibrils, exhibits an enhancement in the fluorescence intensity with an emission peak at 480 nm.[50] Different protein concentrations ranging from 100 to 300 μM,

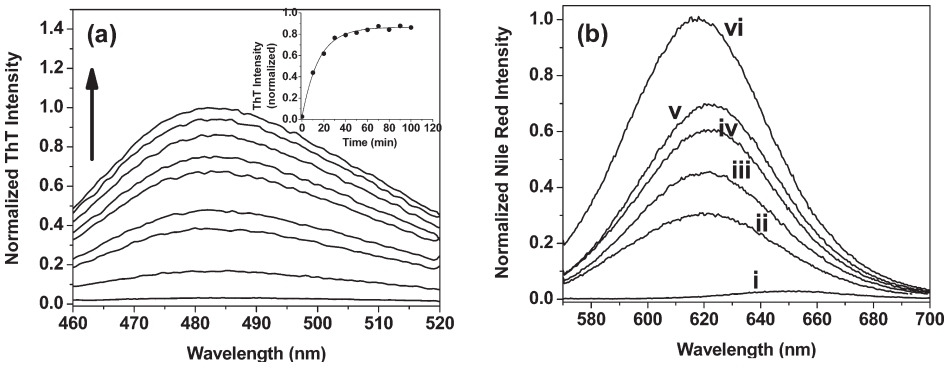

Figure 2. Amyloid aggregation of BSA at pH 3, 50 mM NaCl, and 65 °C monitored by change in ThT and Nile red fluorescence. (a) Evolution of ThT emission spectra as a function of time: inset graph depicts the change in ThT intensity as a function of time at pH 3 and 50 mM NaCl. (b) Change in Nile red fluorescence emission spectra in (i) water; (ii) BSA (10 μM), pH 7; (iii) BSA (10 μM), pH 3; (iv) BSA (100 μM), pH 7; (v) BSA (100 μM), pH 3; and (vi) amyloid fibrils of BSA at pH 3, 65 °C. Spectra ii−vi were collected in the presence of 50 mM NaCl.

incubated with 50 mM NaCl at pH 3, were heated to 65 °C, and the ThT fluorescence intensity of the samples was recorded at regular intervals (for experimental details, see Experimental Methods).[51] Figure 2a shows a typical evolution of ThT fluorescence spectra as a function of time, indicating the formation of amyloid-like aggregates. The plot at pH 3 (Figure 2a inset) reveals that the ThT intensity increased very sharply within the first 10 min of heating, approached a quasi-plateau region in 30 min, and then appeared to be completed within an hour. Approximately, 40-fold enhancement in the ThT fluorescence intensity was observed at the end of fibrillation compared to the intensity observed before the sample was incubated at 65 °C, which indicated the formation of β-sheet-rich amyloid-like aggregates and, hence, an increase in ThT-binding sites. However, it is interesting to note that the propensity of amyloid fibrillation of different conformational isomers of the all α-helical protein appears to be slower at all other pH except at pH 3 (see Figure 3a; the details of the kinetics are discussed in subsequent text). Hence, the pH for BSA aggregation for subsequent studies was optimized at pH 3.[52]

Nile red has been reported as a better amyloid aggregation marker compared to ThT, especially, if the aggregation studies are carried out under acidic conditions.[53] At pH 7 (the native monomeric form) and pH 3 (the acid-expanded monomeric form), the fluorescence emission of Nile red was measured at 620 nm, the latter exhibiting a 2-fold excess intensity compared to that of the native BSA. A substantial increment in the Nile red emission was observed for the unheated sample at pH 3 and 50 mM NaCl. Upon heating, a significant enhancement in the Nile red fluorescence was observed with a concomitant blue shift to 615 nm, which is an indicator of the formation of amyloid-like aggregates (Figure 2b).[53] The observations are in good agreement with that obtained from the ThT fluorescence assay. Hence, we used ThT for all our aggregation experiments to monitor amyloid formation.

Figure 3a shows the changes in ThT fluorescence of all the conformational isomers of BSA in the presence of 50 mM NaCl and 100 μM of protein and heated to 65 °C. The fluorescence intensity curves were fitted to a single-exponential function, and the average rate constants were plotted as a function of pH (Figure 3b). It is interesting to note that the apparent average rate constant at pH 3 is the highest ($\sim 67 \times 10^{-3}$ min^{-1}) compared to that measured at all other pH values. At pH 7 and pH 9, the protein aggregation exhibits similar rate constants of $\sim 26 \times 10^{-3}$ and $\sim 22 \times 10^{-3}$ min^{-1}, respectively. Hence, the pH of the following studies was optimized at pH 3 because the kinetic data suggest that a significant population of molten-globule-like conformers at pH 3 accelerates the fibrillation process substantially. The change in ThT fluorescence was also utilized to monitor fibril formation as a function of the ionic strength of the solution. The ionic strength was varied from 0 to 100 mM, and the rate of fibril formation was found to depend on the salt concentration as evidenced by the plots shown in Figure 3d−f. At 100 mM NaCl, the change in the ThT fluorescence intensity was very rapid and saturation was attained very quickly, whereas, at 25 mM NaCl, the change in ThT intensity was quite slow. The kinetics of amyloid fibrillation appears to be the fastest at the highest ionic strength (100 mM of NaCl, $k = \sim 242 \times 10^{-3}$ min^{-1}), a 121-fold excess to that observed without the electrolyte (0 mM NaCl, $k = \sim 2 \times 10^{-3}$ min^{-1}). The observed rates suggest that the salt facilitates the formation of amyloid-like aggregates, which is consistent with the previously reported data on HSA fibrillation.[34,38] Hence, to monitor the aggregation of BSA, 50 mM NaCl and pH 3 were set as the optimum condition and the following experiments reported herein were carried out under this experimental condition. In all instances, amyloid formation occurs without the presence of any lag-phase, which agrees well with a recent report on the amyloidosis of HSA under similar experimental conditions.[34,37] The amyloid fibrillation of BSA at pH 3 and 50 mM NaCl was monitored by ThT fluorescence as a function of temperature. The apparent rate of amyloid-like aggregate formation was found to be faster at higher temperature, and a linear Arrhenius plot was observed when the observed rate constant was plotted vs $1/T$ (Figure S1 in the Supporting Information). The activation energy was determined to be ~109 kJ/mol, which is close to the reported data for aggregation of other proteins.[35,54] The structures of the BSA fibrils formed under acidic conditions were examined under transmission electron microscope (TEM). The TEM images (Figure 4) revealed infinite stretches (on the order of micrometers) of a flat-ribbon and long-rod-shaped, self-assembled fibrillar network intertwined together.

Next, we carried out experiments to probe the changes in both protein conformation and size during the fibrillation event. We directed our efforts to delineate the sequence of events, especially the early steps, in the amyloid fibrillation cascade. In the

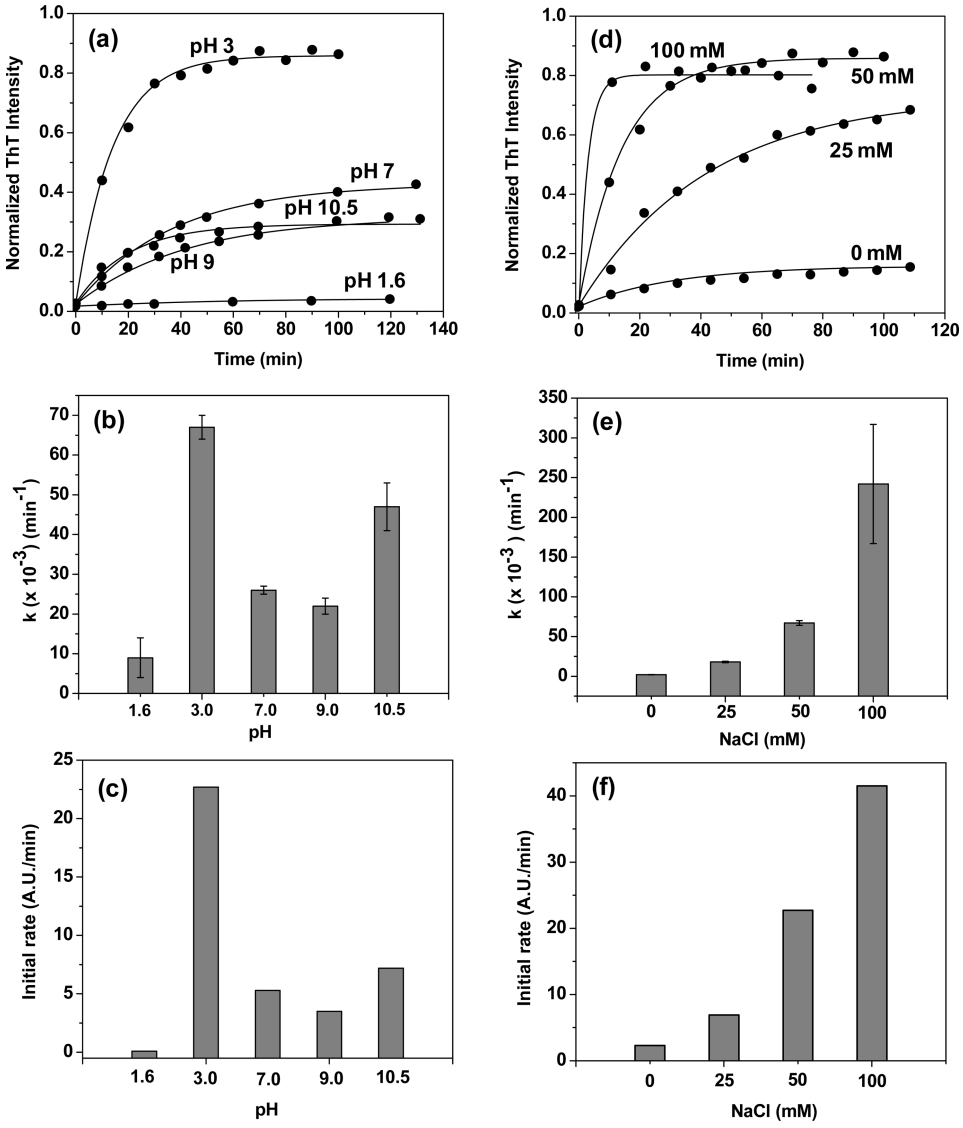

Figure 3. ThT fluorescence kinetics at different pH (a−c) and at different salt concentrations (d−f) during amyloid fibrillation of BSA at 65 °C. The data points at 0 min represent ThT intensity at room temperature prior to heating. Panels a and d show time-dependent changes in ThT intensity fitted by monoexponential functions (solid line), b and e represent the apparent rate constants obtained from aggregation kinetics, and c and f represent the initial rates of aggregation at different pH and salt concentrations, respectively.

following sections, we describe the spectroscopic observations accompanied by a detailed kinetic analysis of multiple structural probes to shed light into the plausible molecular mechanism of BSA fibrillation. In this set of experiments, we have carried out aggregation studies under exactly identical conditions using spectroscopic probes such as tryptophan fluorescence, ANS fluorescence, and CD, which are indicators of conformational changes occurring during aggregation. Additionally, fluorescence anisotropies of tryptophan, ANS, and AEDANS were measured which are the reporters of overall aggregate size growth that occur simultaneously with the conformational changes. Single-exponential kinetics function was able to satisfactorily describe the time-dependent changes of various probes used, and the average rate constants were recovered from the analysis.

3.2. Aggregation Monitored by Tryptophan Fluorescence. The changes in the average fluorescence intensity and anisotropy of the two intrinsic tryptophan residues were monitored during fibrillation as a function of time. At a high protein concentration, 50 mM NaCl, and room temperature, an intense tryptophanyl fluorescence at ∼344 nm was observed which indicates that the tryptophans are present in nonpolar environment. Upon heating to 65 °C, a progressive reduction in tryptophan fluorescence intensity (Figure 5a) accompanied by a slight blue shift (∼3 nm) (Figure S2a,b in Supporting Information) was observed upon formation of the amyloid-like aggregates. We suggest that the observed drop in fluorescence intensity could be either due to (i) exposure of tryptophans to the solvent and/or (ii) quenching of tryptophan intensity due to an increase in the number of phenylalanines, histidines, and disulfides in the proximity of tryptophans that quench the emission upon aggregation mediated by both electrostatic and hydrophobic interactions. Kinetic analysis of the reduction in tryptophan fluorescence intensity yielded an average rate constant of ∼188 × 10^{-3} min^{-1}, which is ∼2.8-fold higher than that of the ThT fluorescence-monitored kinetics (k = ∼ 67 × 10^{-3} min^{-1}) observed under identical conditions. Prior to heating at 65 °C, a

dx.doi.org/10.1021/jp111528c |J. Phys. Chem. B 2011, 115, 4195–4205

small but measurable increase in tryptophan fluorescence anisotropy was observed as compared to that of the monomeric protein in pH 3. This could probably be attributed to the formation of soluble oligomers at higher protein concentration from the acid-expanded conformer of BSA whereby the oligomerization could be facilitated by the presence of salt. To further verify oligomerization, the changes in scattering and fluorescence polarization properties of BSA as a function of protein concentration at pH 3 and 50 mM NaCl were investigated. The results suggested that BSA, indeed, forms soluble oligomers at a concentration of 100 μM (Figure S3 in Supporting Information).[55] A significant enhancement in the tryptophan fluorescence anisotropy without any lag phase was observed upon heating that reached saturation very quickly as fibrillation progressed, suggesting formation of large-sized aggregates (Figure 5a). The apparent rate constant obtained for changes in tryptophan anisotropy was $\sim 97 \times 10^{-3}$ min^{-1}. Comparison of the two rate constants, monitored by tryptophan fluorescence, reveals that the conformational changes occur at a faster rate compared to that of the overall size growth of the aggregates.

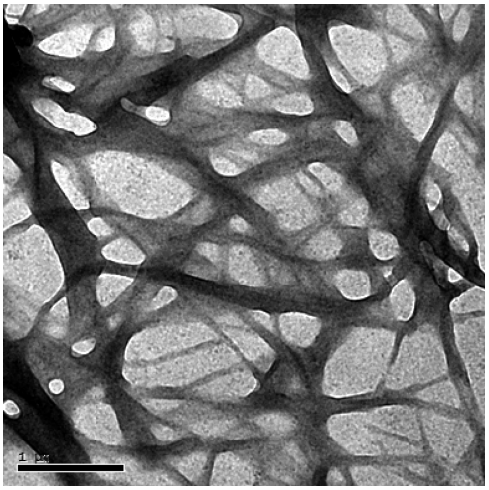

Figure 4. TEM image of BSA fibrils formed at pH 3, 50 mM NaCl, and 65 °C after heating for 4 h followed by a 30 days long incubation at room temperature (25 °C). Scale bar: 1 μm.

3.3. Aggregation Monitored by ANS Fluorescence. To determine whether hydrophobic regions are accessible and attainable in the oligomerization and subsequent amyloid fibrillation of protein at pH 3, the fluorescence intensity and anisotropy of ANS were measured. ANS is an extrinsic fluorophore which is weakly fluorescent in aqueous environment but fluoresces strongly (with a concurrent blue shift in its emission maximum from ~515 to ~475 nm) when located in a hydrophobic environment.[56] Recently, it has been demonstrated that the change in ANS fluorescence intensity during protein self-assembly can be correlated to the cytotoxicity of the amyloidogenic species.[57] In our experiments, ANS was initially bound to the hydrophobic pockets and charged surface residues of the unheated sample at pH 3. After the temperature jump, a sharp enhancement in the ANS emission at 475 nm (Figure S2c in the

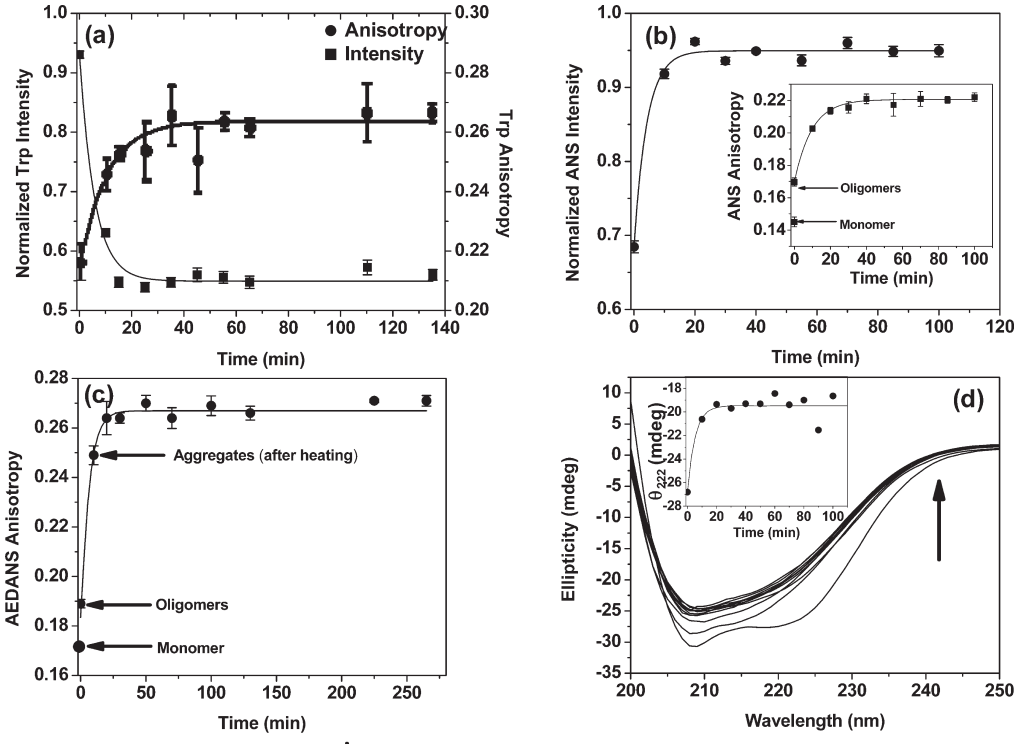

Figure 5. Conformational and size changes occurring during amyloid fibrillation of BSA at pH 3, 50 mM NaCl, 65 °C as a function of time monitored by (a) tryptophan fluorescence intensity and anisotropy, (b) ANS fluorescence intensity and anisotropy (inset), (c) AEDANS fluorescence anisotropy, and (d) secondary structural changes monitored by far-UV CD spectra and change in ellipticity at 222 nm as a function of time (inset). The data points at 0 min represent fluorescence intensity and anisotropy of the respective structural probe at 25 °C, i.e., prior to heating. The solid lines represent the fit obtained from monoexponential function. All of the experiments were repeated several times separately and were highly reproducible.

dx.doi.org/10.1021/jp111528c |J. Phys. Chem. B 2011, 115, 4195–4205

Supporting Information) followed by a plateau was observed which indicated a dramatic increase in the extent of hydrophobic environment (Figure 5b). Kinetic analysis of the ANS fluorescence intensity data yielded an apparent rate constant of ~244 × 10^{-3} min^{-1}, slightly faster (~1.3 times) than that of the tryptophanyl fluorescence kinetics. Therefore, a blue shift in tryptophan emission and a sharp increase in ANS fluorescence intensity indicate a rise in the nonpolar environment or hydrophobicity upon heating that drives the oligomerization−fibrillation reaction. At room temperature and higher protein concentration, the ANS fluorescence anisotropy was higher (0.17 ± 0.002) compared to that of the monomeric protein (0.14 ± 0.003), suggesting the existence of soluble oligomers. Upon heating to 65 °C, the ANS anisotropy showed a monotonic increase and attained saturation after 40 min of heating (see Figure 5b inset) and exhibited an average rate constant of ~102 × 10^{-3} min^{-1}, almost similar to that of the tryptophan fluorescence anisotropy. These observations taken together suggest that higher protein concentration induces a collapse of the hydrophobic patches in an otherwise expanded, molten-globule-like form of the α-helical protein which is aided by the addition of salt at room temperature. During the temperature jump, both the salt and temperature placate the formation and growth of larger aggregates with increased hydrophobicity (reflected in the rise in fluorescence intensity and anisotropy) which eventually form amyloid-like fibrillar aggregates. Here again, similar to tryptophan fluorescence kinetics, the rate of change in conformation, and, hence, hydrophobicity monitored by ANS, is much faster than that of the overall size growth.

3.4. Aggregation Monitored by AEDANS Fluorescence. We have reported earlier that the far-UV CD spectrum of the monomeric protein indicated a considerable loss in helical content at pH 3 which was correlated to the loss of intradomain helicity in domains I and II from the FRET efficiency data.[48] Additionally, the findings obtained from tryptophan and ANS fluorescence suggest that, at room temperature, the molten-globule-like isomer collapses to hydrophobic-rich oligomers at higher protein concentration and salt which eventually leads to larger aggregates. Therefore, to decipher the plausible involvement of domain I (largely disordered at pH 3) in oligomerization and amyloid fibrillation, the following studies were carried out. The availability of a single, free cysteine residue (Cys34) in domain I of the α-helical protein under the present study provides us with a unique advantage of carrying out a chemical modification of the cysteine. IAEDANS was employed to label the thiol group of the cysteine residue (for details, see Experimental Methods) specifically because IAEDANS has a long fluorescence lifetime,[47] so any small change in the conformation and size can be easily and clearly detected within the lifetime of this probe. Aggregation of labeled BSA (5% of the total BSA concentration) was monitored by AEDANS fluorescence anisotropy under the same acidic conditions in the presence of NaCl (Figure 5c). The initial fluorescence anisotropy of BSA−AEDANS (before heating) was found to be 0.19 ± 0.004, again suggesting the existence of soluble oligomers (anisotropy of BSA−AEDANS monomer at pH 3 was 0.17 ± 0.002), which enhanced rapidly upon heating and reached saturation at a value of ~0.26. It should be noted here that the covalently labeled cysteine is located in domain I; hence, the observed changes in the fluorescence anisotropy of AEDANS can be correlated with only a local structural reordering of domain I. Interestingly, the apparent rate constant obtained from the changes in AEDANS fluorescence anisotropy is ~142 × 10^{-3} min^{-1}, which is much faster (~1.5 times) than that obtained from ANS and tryptophan anisotropies, respectively, but, again, slower than the conformational changes. Overall, the AEDANS fluorescence anisotropy data imply that the partially exposed domains in the molten-globule-like form of BSA, under mildly acidic conditions, form amyloid-like aggregates wherein the sequestration of domain I into hydrophobic oligomers is one of the earliest events that takes place during the fibrillation process. Moreover, the covalently labeled cysteine residue did not appear to obstruct the fibril formation, which is congruent with a previous report.[35]

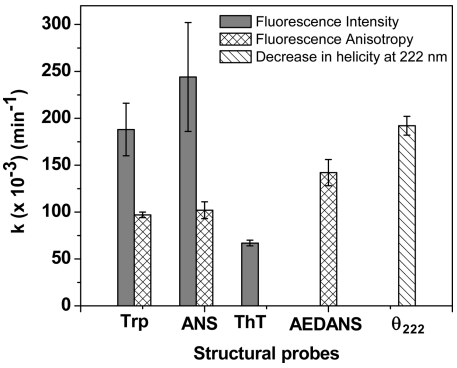

Figure 6. Comparison of the rate constants of amyloid fibrillation kinetics of multiple structural probes as depicted by changes in conformation and size to delineate the steps involved in the fibrillation event.

3.5. Aggregation Monitored by CD Spectroscopy. At pH 3 and 50 mM NaCl, the far-UV CD spectrum of BSA shows minima at 222 and 209 nm, which is a characteristic of an α-helix rich protein. After the sample was incubated at 65 °C, there was a successive loss in the helicity at 222 and 209 nm as revealed by the far-UV CD spectra (Figure 5d) which may suggest that the formation of both β-sheet and unordered conformation occur at the expense of helical conformation. This also implies that partially unfolded conformers having variable secondary structural contents exist in solution after heating which subsequently lead to the formation of β-sheet-rich amyloid aggregates as evidenced by an increase in ThT and Nile red fluorescence. The average rate constant of loss of helicity at 222 nm (inset of Figure 5d) was determined to be ~192 × 10^{-3} min^{-1}, almost equal to that of the tryptophanyl and ANS fluorescence intensity kinetics and corroborates the changes in conformations at a faster rate compared to the overall size growth.

All these observations and kinetic analyses suggest that though the aggregation is devoid of nucleation step and appears to progress continuously, discrete crucial events, especially the earliest ones, pertaining to the aggregation could be traced in a time-dependent manner. The initial rise in fluorescence anisotropy of the structural probes at room temperature indicated that, at a higher protein concentration, oligomerization occurs which is facilitated by the presence of salt. Figure 6 depicts a comparison between the rate of conformational changes and that of the overall size growth, which suggests that the conformational conversion in the preformed oligomers occurs considerably faster than the growth of higher order aggregates. Association of these aggregates subsequently leads to the formation of amyloid-like fibrils with increasing β-sheet content.

4. DISCUSSION

The prevailing concept in the amyloid biology is that fibrillation is a generic property of a polypeptide chain and the amyloid fibril comprises a "cross-β" structure regardless of the distinct amino acid sequence pattern which is encoded in the polypeptide.[10] The studies involving formation of amyloid fibrils at neutral pH is extremely important since numerous amyloid-related pathogeneses have been identified under similar conditions. Nevertheless, there are certain nonneutral conditions that also play an important role in physiological functions; e.g., low-pH regions are encountered near the cell membrane surfaces.[31] Therefore, carrier proteins such as serum albumins, that transport and release a variety of substrates and drugs in the bloodstream, come in contact with low-pH regions frequently. Additionally, serum albumins are themselves responsible for the maintenance of blood pH,[23] and combined with the fact that they form reversible conformational isomers depending on the pH,[30] it is both important and interesting to study their aggregation propensity under low-pH conditions. Moreover, it has been pointed out that destabilization of the native state is a key to aggregation or fibrillation;[12] therefore, lowering the pH and/or raising the temperature aids in significant accumulation of partially unfolded conformational populations that are otherwise inaccessible in their native forms. We have studied the aggregation propensity of different conformational isomers of an all α-helical protein in the presence of salt and observed that one of the conformational isomers, formed at pH 3, predominantly forms amyloid-like aggregates at 50 mM NaCl when heated to 65 °C. A variety of methodologies probing both conformation and size changes have been employed to get insights into the mechanistic aspects of amyloid fibrillation of BSA. Although the aggregation reactions are endowed with inherent complexity, all of the kinetic traces could be fitted to a single-exponential function. However, the interpretation and comparison of the apparent rate constants of aggregation at different pH is a difficult proposition as the aggregation reactions are fairly complex in nature, because they might lead to the formation of different structural intermediates and morphologically distinct aggregates depending on the solution conditions.[9,16,37] The kinetic analysis of the aggregation tendency of different conformational isomers suggests that there could be multiple oligomerization−aggregation pathways which compete with each other and become predominant at a specific pH value and drive the aggregation forward. Nevertheless, the fact that the ThT intensity increases upon heating at all pH indicates that an increase in β-rich amyloid-like aggregates occurs though the extent and rate of formation varies across the pH values studied. The rate of fibrillation is faster in the presence of salt and exhibits a linear relationship when log k is plotted against the square root of the ionic strength (Figure S4 in the Supporting Information). This suggests that the addition of salt screens the repulsion between the protein molecules, thus facilitating aggregation. Also, the higher the concentration of the electrolyte, the better the charge shielding is and the faster the aggregation is .[38] Another important point to note is that the probes used in our study show different rates of conformational changes and assembly during aggregation. This finding is useful in delineating the oligomerization and structural reorganization steps involved in the fibril formation. The sample incubated at 100 μM of BSA remained as a clear solution even after heating for 4 h and keeping at room temperature for a period over days to months indicative of the fact that the oligomers and the subsequent fibrillar aggregates are soluble. It has been pointed out that the soluble oligomers and fibrillar aggregates are cytotoxic and seem to be responsible for the onset of neurodegeneration, whereas fibrils appear to be relatively harmless unless they assemble to very high levels causing organ malfunction and subsequent failure.[58]

There have been several reports that, in the absence of seeding, accruement of oligomeric assemblies drives the spontaneous fibrillation of several proteins under acidic conditions.[37,54,59] As discussed previously, the acid-expanded, molten-globule-like isomer of BSA forms oligomers immediately at high protein concentration and in the presence of salt. Such phenomenon is discernible given the fact that there is a substantial loss in intradomain helicity of domain I when BSA forms an expanded, molten-globule-like state at pH 3,[48] giving rise to a considerable fraction of extended structures. At a higher protein concentration, these exposed, disordered segments (both from domain I and the remaining inherent extended structures) assemble via hydrophobic interactions and form soluble (molten) oligomers at room temperature. This observation is consistent with a recent report on HSA.[37] Additionally, by using a covalently attached, surface-modifying fluorescent probe, rhodamine-B isothiocyanate, it was observed that the fluorescence intensity and anisotropy of rhodamine-B remained unaltered throughout the study. This suggests that the surface residues participate in the overall fibril formation process, which when modified, halts the aggregation.

In our present investigation, various structural probes in tandem were utilized to decipher the temporal evolution of both conformational and size changes during the aggregation (Figure 6 and Table S1). The rate of conformational changes observed by fluorescence (tryptophan and ANS intensities) and CD spectroscopy are almost similar but markedly higher than that monitored by ThT fluorescence. One of the salient features of fluorescence anisotropy kinetics is that the rate of change in AEDANS anisotropy is higher than that of the other two probes (tryptophan and ANS anisotropy), which implies that the sequestration of domain I into the aggregate is likely to be the earliest events in the oligomerization and self-assembly process (Figure 6). However, comparison of the kinetics of conformational changes and fluorescence anisotropy indicate that the rate of conformational change is higher than that of the overall size growth of the aggregates (Figure 6). This indicates that an increasing amount of unordered structures and β-sheets are formed at an expense of α-helices, favored by the salt and elevated temperature, which is also corroborated by our CD data (Figure 5d). We suggest that conformational conversion from α-helices to extended regions and β-sheets in the preformed molten oligomers occurs faster compared to the aggregate size growth and subsequent formation of β-sheet-rich amyloid-like aggregates at higher temperature. The kinetics monitored by ThT-fluorescence is comparable to the anisotropy kinetics probed by different fluorescent markers, which indicates that the size increase and the formation of β-sheet-rich fibrillar aggregates occur simultaneously. Also, ThT appears to be the slowest of all probes used in this study, suggestive of the fact that ThT exhibits the strongest signal when it is bound to mature fibrils.[41]

Typically, fibrillation occurs by a nucleation-dependent polymerization mechanism whereby the fibril formation is preceded by a lag phase and is strongly concentration-dependent, denoting the formation of critical-oligomeric nucleus that facilitates the association and sequestration of other monomers into fibrils.[2,3,60]

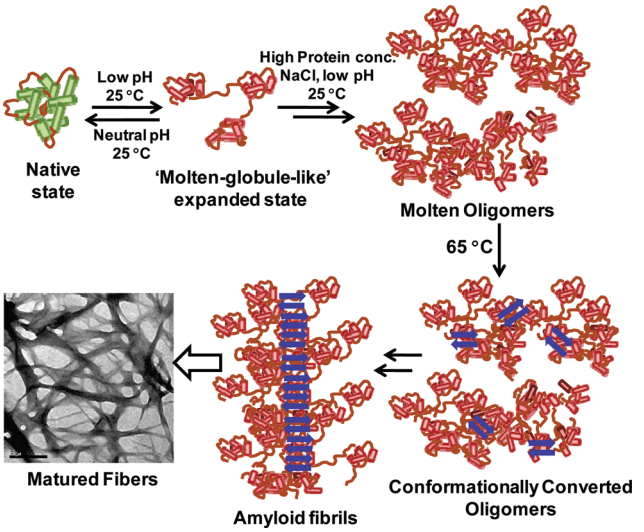

Figure 7. Suggested model for fibril formation from serum albumins.

In our study, a common observation obtained from multiple probes is that the conversion of BSA monomers to fibrils under various pH conditions proceeds without any lag phase (Figures 3 and 5). This observation is in line with the reports on HSA and BSA fibrillation.[34,35] The nonexistent lag phase has been found to be independent of protein concentration and seeding in earlier studies.[35,37] This suggests that BSA fibrillation neither solely follows the classical nucleated polymerization kinetics[60] nor is dominated by the secondary nucleation phenomenon.[61] The characteristic absence of a lag phase has also been demonstrated in the amyloidogenesis of acylphosphatase,[10] β_2-microglobulin,[62,63] transthyretin,[64] prion protein,[54] and barstar.[65] The absence of a lag phase has been attributed to the formation of "propagation-competent nucleus-like structures"[35] that do not require the formation of high-energy, critical-and-unstable nucleus.[64] Such a phenomenon can be explained by a few available kinetic models such as "random association",[66] "supercritical concentration driven fibril formation",[67] and "downhill polymerization".[68] Given the inherent complex nature of aggregation kinetics,[69] although it is difficult to assign any particular kinetic pathway for serum albumin fibrillation, we speculate that the overall kinetics observed is a complex combination of either some or all of the three "lag-phase-independent" mechanisms mentioned above. Complete kinetic analyses of protein aggregation processes have yielded several prominent models such as template assembly,[69,70] monomer-directed conversion,[71] nucleated polymerization,[72−74] and nucleated conformational conversion (NCC).[75] The NCC model states that the conformational conversion occurs within the "molten" oligomeric intermediate and forms nuclei that drive the assembly rapidly. In our case, we suggest a plausible molecular mechanism of BSA fibrillation (Figure 7) that mostly echoes the central theme of the NCC model, while incorporating the features of both downhill and irreversible polymerization to account for the absence of a lag phase. At room temperature and low pH, the protein forms a molten-globule-like state that gives rise to exposed hydrophobic regions at a low protein concentration.[48] An increase in the protein concentration induces (intermolecular) self-association whereby domain I is sequestered into the oligomers. At elevated temperature, a conformational conversion from α-helix and random coil structures to β-rich structures is facilitated in these preformed oligomers that serve as precursors of matured amyloid fibrils. In summary, our present investigation reveals multiple and kinetically distinct steps such as conformational changes (fluorescence intensity and CD) and size changes (fluorescence anisotropy) followed by fibril formation (ThT binding) as depicted in a simplistic model (Figure 7).

5. CONCLUSION

Our results presented here demonstrate that the acid-expanded, molten-globule-like isomer[48] of an all α-helical protein such as BSA forms amyloid-like fibrils under carefully designed conditions. By using spectroscopic techniques, we have been able to delineate the early steps that are involved in the fibrillation event. The molten-globule-like conformational isomer becomes significantly populated at pH 3 and forms a "propagation-competent nucleus" at higher protein concentration. The conformational rearrangement in the early (molten) oligomers precedes the formation of larger aggregates, leading to the formation of β-rich fibrils. The mechanistic insights gained from the present work would be useful in the design of antiamyloid therapeutics by targeting various stages of the aggregation process. Additionally, we believe that the combination of methodologies used in this work will find broad application in the study of misfolding and aggregation of other physiologically important proteins.

■ ASSOCIATED CONTENT

Ⓢ Supporting Information. Figures S1−S4 and Table S1 showing changes in fluorescence properties of different probes used in this study to characterize BSA aggregation. This material is available free of charge via the Internet at http://pubs.acs.org.

■ AUTHOR INFORMATION

Corresponding Author
*E-mail: mukhopadhyay@iisermohali.ac.in.

■ ACKNOWLEDGMENT

We thank IISER Mohali for the financial support during the course of the present investigation. M.B. thanks the Department of Science and Technology (DST) Women Scientists' Scheme for partial support toward research fellowship. We also thank Mr. Supratim Banerjee (IISc Bangalore) for recording the TEM images, the Guptasarma Laboratory (IMTECH Chandigarh) for helping us with the CD measurements and Dr. Kausik Chattopadhyay (IISER Mohali) for valuable comments on this manuscript.

■ REFERENCES

(1) Luheshi, L. M.; Crowther, D. C.; Dobson, C. M. Protein misfolding and disease: From the test tube to the organism. *Curr. Opin. Chem. Biol.* **2008**, *12*, 25–31.

(2) Jahn, T. R.; Radford, S. E. Folding versus aggregation: Polypeptide conformations on competing pathways. *Arch. Biochem. Biophys.* **2008**, *469*, 100–117.

(3) Wetzel, R. Kinetics and thermodynamics of amyloid fibril assembly. *Acc. Chem. Res.* **2006**, *39*, 671–679.

(4) Pepys, M. B. Amyloidosis. *Annu. Rev. Med.* **2006**, *57*, 223–241.

(5) Miranker, A. D. Unzipping the mysteries of amyloid fiber formation. *Proc. Natl. Acad. Sci. U.S.A.* **2004**, *101*, 4335–4336.

(6) Tycko, R. Progress towards a molecular level structural understanding of amyloid fibrils. *Curr. Opin. Struct. Biol.* **2004**, *14*, 96–103.
(7) Rochet, J. C.; Lansbury, P. T., Jr. Amyloid fibrillogenesis: Themes and variations. *Curr. Opin. Struct. Biol.* **2000**, *10*, 60–68.
(8) Gazit, E. Mechanisms of amyloid fibril self-assembly and inhibition: Model short peptides as a key research tool. *FEBS J.* **2005**, *272*, 5971–5978.
(9) Guijarro, J. I.; Sunde, M.; Jones, J. A.; Campbell, I. D.; Dobson, C. M. Amyloid fibril formation by an SH3 domain. *Proc. Natl. Acad. Sci. U.S.A.* **1998**, *95*, 4224–4228.
(10) Chiti, F.; Webster, P.; Taddei, N.; Clark, A.; Stefani, M.; Ramponi, G.; Dobson, C. M. Designing conditions for in vitro formation of amyloid protofilaments and fibrils. *Proc. Natl. Acad. Sci. U.S.A.* **1999**, *96*, 3590–3594.
(11) Fandrich, M.; Fletcher, M. A.; Dobson, C. M. Amyloid fibrils from muscle myoglobin. *Nature* **2001**, *410*, 165–166.
(12) Uversky, V. N.; Fink, A. L. Conformational constraints for amyloid fibrillation: The importance of being unfolded. *Biochim. Biophys. Acta* **2004**, *1698*, 131–153.
(13) Kelly, J. W. The alternative conformations of amyloidogenic proteins and their multi-step assembly pathways. *Curr. Opin. Struct. Biol.* **1998**, *8*, 101–106.
(14) Zerovnik, E. Amyloid-fibril formation, proposed mechanisms and relevance to conformational disease. *Eur. J. Biochem.* **2002**, *269*, 3362–3371.
(15) Morel, B.; Casares, S.; Conejero-Lara, F. A. Single mutation induces amyloid aggregation in the α-spectrin SH3 domain: Analysis of the early stages of fibril formation. *J. Mol. Biol.* **2006**, *356*, 453–468.
(16) Chiti, F.; Taddei, N.; Baroni, F.; Capanni, C.; Stefani, M.; Ramponi, G.; Dobson, C. M. Kinetic partitioning of protein folding and aggregation. *Nat. Struct. Biol.* **2002**, *9*, 137–143.
(17) Chiti, F.; Stefani, M.; Taddei, N.; Ramponi, G.; Dobson, C. M. Rationalization of the effects of mutations on peptide and protein aggregation rates. *Nature* **2003**, *424*, 805–808.
(18) Volles, M. J.; Lee, S.-J.; Rochet, J.-C.; Shtilerman, M. D.; Ding, T. T.; Kessler, J. C.; Lansbury, P. T. Vesicle permeabilization by protofibrillar α-synuclein: Implications for the pathogenesis and treatment of Parkinson's disease. *Biochemistry* **2001**, *40*, 7812–7819.
(19) Kayed, R.; Sokolov, Y.; Edmonds, B.; McIntire, T. M.; Milton, S. C.; Hall, J. E.; Glabe, C. G. Permeabilization of lipid bilayers is a common conformation-dependent activity of soluble amyloid oligomers in protein misfolding diseases. *J. Biol. Chem.* **2004**, *279*, 46363–46366.
(20) Bucciantini, M.; Giannoni, E.; Chiti, F.; Baroni, F.; Formigli, L.; Zurdo, J.; Taddei, N.; Ramponi, G.; Dobson, C. M.; Stefani, M. Inherent toxicity of aggregates implies a common mechanism for protein misfolding diseases. *Nature* **2002**, *416*, 507–511.
(21) Herczenik, E.; Gebbink, M. F. B. G. Molecular and cellular aspects of protein misfolding and disease. *FASEB J.* **2008**, *22*, 2115–2133.
(22) Davis, T. J.; Soto-Ortega, D. D.; Kotarek, J. A.; Gonzalez-Velasquez, F. J.; Sivakumar, K.; Wu, L.; Wang, Q.; Moss, M. A. Comparative study of inhibition at multiple stages of amyloid-β self-assembly provides mechanistic insight. *Mol. Pharmacol.* **2009**, *76*, 405–413.
(23) Carter, D. C.; Ho, J. X. Structure of serum albumin. *Adv. Protein Chem.* **1994**, *45*, 153–203.
(24) Peters, T., Jr. Serum albumin. *Adv. Protein Chem.* **1985**, *37*, 161–245.
(25) Rossing, T. H.; Maffaeo, N.; Fencl, V. Acid−base effects of altering plasma protein concentration in human blood in vitro. *J. Appl. Physiol.* **1986**, *61*, 2260–2265.
(26) He, X. M.; Carter, D. C. Atomic structure and chemistry of human serum albumin. *Nature* **1992**, *358*, 209–215.
(27) Sugio, S.; Kashima, A.; Mochizuki, S.; Noda, M.; Kobayashi, K. Crystal structure of human serum albumin at 2.5Å resolution. *Protein Eng.* **1999**, *12*, 439–446.
(28) Luetscher, J. A. Serum albumin. II. Identification of more than one albumin in horse and human serum by electrophoretic mobility in acid solution. *J. Am. Chem. Soc.* **1939**, *61*, 2888–2890.
(29) Williams, E. J.; Foster, J. F. The aggregation of bovine plasma albumin at low pH. *J. Am. Chem. Soc.* **1960**, *82*, 3741–3745.
(30) Foster, J. F. Some aspects of the structure and the conformational properties of serum albumin. In *Albumin structure, function and uses*; Rosenoer, V. M., Oratz, M., Rothschild, M. A., Eds.; Pergamon: Oxford, U.K., 1977; pp 53−84.
(31) Wilting, J.; Kremer, J. M. H.; Ijzerman, A. P.; Schulman, S. G. The kinetics of the binding of warfarin to human serum albumin as studied by stopped-flow spectrophotometry. *Biochim. Biophys. Acta* **1982**, *706*, 96–104.
(32) Militello, V.; Vetri, V.; Leone, M. Conformational changes involved in thermal aggregation processes of bovine serum albumin. *Biophys. Chem.* **2003**, *105*, 133–141.
(33) Militello, V.; Casarino, C.; Emanuele, A.; Giostra, A.; Pullara, F.; Leone, M. Aggregation kinetics of bovine serum albumin studied by FTIR spectroscopy and light scattering. *Biophys. Chem.* **2004**, *107*, 175–187.
(34) Taboada, P.; Barbosa, S.; Castro, E.; Mosquera, V. Amyloid fibril formation and other aggregate species formed by human serum albumin association. *J. Phys. Chem. B* **2006**, *110*, 20733–20736.
(35) Holm, N. K.; Jespersen, S. K.; Thomassen, L. V.; Wolff, T. Y.; Sehgal, P.; Thomsen, L. A.; Christiansen, G.; Andersen, C. B.; Knudsen, A. D.; Otzen, D. E. Aggregation and fibrillation of bovine serum albumin. *Biochim. Biophys. Acta* **2007**, *1774*, 1128–1138.
(36) Vetri, V.; Librizzi, F.; Leone, M.; Militello, V. Thermal aggregation of bovine serum albumin at different pH: Comparison with human serum albumin. *Eur. Biophys. J.* **2007**, *36*, 717–725.
(37) Juarez, J.; Taboada, P.; Mosquera, V. Existence of different structural intermediates on the fibrillation pathway of human serum albumin. *Biophys. J.* **2009**, *96*, 2353–2370.
(38) Juarez, J.; Lopez, S. G.; Cambon, A.; Taboada, P.; Mosquera, V. Influence of electrostatic interactions on the fibrillation process of human serum albumin. *J. Phys. Chem. B* **2009**, *113*, 10521–10529.
(39) Sanghamitra, N. J. M.; Varghese, N.; Rao, C. N. R. Effect of curcumin and Cu^{2+}/Zn^{2+} ions on the fibrillar aggregates formed by the amyloid peptide and other peptides at the organic-aqueous interface. *Chem. Phys. Lett.* **2010**, *496*, 104–108.
(40) Wei, Y.; Chen, L.; Chen, J.; Ge, L.; He, R. Q. Rapid glycation with D-ribose induces globular amyloid-like aggregations of BSA with high cytotoxicity to SH-SY5Y cells. *BMC Cell Biol.* **2009**, 10, doi:10.1186/1471-2121-10-10.
(41) Lindgren, M.; Sörgjerd, K.; Hammarström, P. Detection and characterization of aggregates, prefibrillar amyloidogenic oligomers and protofibrils using fluorescence spectroscopy. *Biophys. J.* **2005**, *88*, 4200–4212.
(42) Allsop, D.; Swanson, L.; Moore, S.; Davies, Y.; York, A.; El-Agnaf, O. M. A.; Soutar, I. Fluorescence anisotropy: A method for early detection of Alzheimer β-peptide (A-β) aggregation. *Biochem. Biophys. Res. Commun.* **2001**, *285*, 58–63.
(43) Mukhopadhyay, S.; Nayak, P. K.; Udgaonkar, J. B.; Krishnamoorthy, G. Characterization of the formation of amyloid protofibrils from barstar by mapping residue-specific fluorescence dynamics. *J. Mol. Biol.* **2006**, *358*, 935–942.
(44) Dusa, A.; Kaylor, J.; Edridge, S.; Bodner, N.; Hong, D.-P.; Fink, A. L. Characterization of oligomers during α-Synuclein aggregation using intrinsic tryptophan fluorescence. *Biochemistry* **2006**, *45*, 2752–2760.
(45) Padrick, S. B.; Miranker, A. D. Islet amyloid: Phase partitioning and secondary nucleation are central to the mechanism of fibrillogenesis. *Biochemistry* **2002**, *41*, 4694–4703.
(46) Atanasiu, C.; Su, T.-J.; Sturrock, S. S.; Dryden, D. T. F. Interaction of the ocr gene 0.3 protein of bacteriophage T7 with EcoKI restriction/modification enzyme. *Nucleic Acids Res.* **2002**, *30*, 3936–3944.
(47) Hudson, E. N.; Weber, G. Synthesis and characterization of two fluorescence sulfhydryl reagents. *Biochemistry* **1973**, *12*, 4154–4161.
(48) Bhattacharya, M.; Jain, N.; Bhasne, K.; Kumari, V.; Mukhopadhyay, S. pH-induced conformational isomerization of bovine serum albumin

studied by extrinsic and intrinsic protein fluorescence. *J. Fluoresc.* (Published online Dec. 3, **2010**; DOI: 10.1007/s10895-010-0781-3).

(49) Lakowicz, J. R. *Principles of fluorescence spectroscopy*, 3rd ed.; Springer: New York, 2006.

(50) Levine, H., III. Quantification of β-sheet amyloid fibril structures with thioflavin T. *Methods Enzymol.* **1999**, *309*, 274–284.

(51) The sample incubated at 300 μM BSA and 50 mM NaCl coagulated and formed a white gel within 5 min of heating, which restricted us from recording the progressive changes in ThT intensity further during the time course of aggregation.

(52) Aggregation at pH 3.5 and 5 under identical incubation conditions could not be monitored since, in the former, the protein became increasingly turbid with time upon heating that resulted in an inconsistent, oscillating pattern in the ThT fluorescence intensity. For the sample incubated at pH 5, the protein coagulated within 4 min of heating, which could be accounted for the fact that pH 5 is very close to the isoelectric point (pI = 4.5−4.8) of BSA, implying that the aggregation mechanism is "more disordered" wherein larger aggregates add onto the smaller ones (see ref 36).

(53) Mishra, R.; Sörgjerd, K.; Nyström, S.; Nordigården, A.; Yu, Y.-C.; Hammarström, P. Lysozyme amyloidogenesis is accelerated by specific nicking and fragmentation but decelerated by intact protein binding and conversion. *J. Mol. Biol.* **2007**, *366*, 1029–1044.

(54) Jain, S.; Udgaonkar, J. B. Evidence for stepwise formation of amyloid fibrils by the mouse prion protein. *J. Mol. Biol.* **2008**, *382*, 1228–1241.

(55) Although the steady-state fluorescence anisotropy does not allow us to determine the exact oligomeric size and the aggregation number, it is likely that the initial oligomers are not very large since none of the fluorescent reporters exhibited a large increase in the anisotropy upon oligomer formation. Subsequently, these small oligomers grew in size during fibril formation as indicated by a large increase in the anisotropy.

(56) Daniel, E.; Weber, G. Cooperative effects in binding by bovine serum albumin I: The binding of 1-anilino-8-naphthalenesulfonate fluorimetric titrations. *Biochemistry* **1966**, *5*, 1893–1900.

(57) Bolognesi, B.; Kumita, J. R.; Barros, T. P.; Esbjorner, E. K.; Luheshi, L. M.; Crowther, D. C.; Wilson, M. R.; Dobson, C. M.; Favrin, G.; Yerbury, J. J. ANS binding reveals common features of cytotoxic amyloid species. *ACS Chem. Biol.* **2010**, *5*, 735–740.

(58) Pepys, M. B.; Hawkins, P. H.; Booth, D. R.; Vigushin, D. M.; Tennent, G. A.; Soutar, A. K.; Totty, N.; Bguyen, O.; Blake, C. C.; Terry, C. J.; Feest, T. G.; Zalin, A. M.; Hsuan, J. J. Human lysozyme gene mutations cause hereditary systemic amyloidosis. *Nature* **1993**, *362*, 553–557.

(59) Harper, J. D.; Lansbury, P. T., Jr. Models of amyloid seeding in Alzheimer's disease and scrapie: Mechanistic truths and physiological consequences of the time-dependent solubility of amyloid proteins. *Annu. Rev. Biochem.* **1997**, *66*, 385–407.

(60) Oosawa, F.; Asakura, S.; Hotta, K.; Nobuhisa, I.; Ooi, T. G-F transformation of actin as a fibrous condensation. *J. Polym. Sci.* **1959**, *37*, 323–336.

(61) Knowles, T. P. J.; Waudby, C. A.; Devlin, G. L.; Cohen, S. I. A.; Aguzzi, A.; Vendruscolo, M.; Terentjev, E. M.; Welland, M. E.; Dobson, C. M. An analytical solution to the kinetics of breakable filament assembly. *Science* **2009**, *326*, 1533–1537.

(62) Radford, S. E.; Gosal, W. S.; Platt, G. W. Towards an understanding of the structural and molecular mechanism of β2-microglobulin amyloid formation in vitro. *Biochim. Biophys. Acta* **2005**, *1753*, 51–63.

(63) Sasahara, K.; Yagi, H.; Sakai, M.; Naiki, H.; Goto, Y. Amyloid nucleation triggered by agitation of β2-microglobulin under acidic and neutral pH conditions. *Biochemistry* **2008**, *47*, 2650–2660.

(64) Hurshman, A. R.; White, J. T.; Powers, E. T.; Kelly, J. W. Transthyretin aggregation under partially denaturing conditions is a downhill polymerization. *Biochemistry* **2004**, *43*, 7365–7381.

(65) Kumar, S.; Mohanty, S. K.; Udgaonkar, J. B. Mechanism of formation of amyloid protofibrils of barstar from soluble oligomers: Evidence for multiple steps and lateral association coupled to conformational conversion. *J. Mol. Biol.* **2007**, *367*, 1186–1204.

(66) Thusius, D.; Dessen, P.; Jallon, J.-M. Mechanism of bovine liver glutamate dehydrogenase self-association I. Kinetic evidence for a random association of polymer chains. *J. Mol. Biol.* **1975**, *92*, 413–432.

(67) Powers, E. T.; Powers, D. L. The kinetics of nucleated polymerizations at high concentrations: Amyloid fibril formation near and above the "supercritical concentration". *Biophys. J.* **2006**, *91*, 122–132.

(68) Pappu, R. V.; Wang, X.; Vitalis, A.; Crick, S. L. A polymer physics perspective on driving forces and mechanisms for protein aggregation. *Arch. Biochem. Biophys.* **2008**, *469*, 132–141.

(69) Morris, A. M.; Watzky, M. A.; Finke, R. G. Protein aggregation kinetics, mechanism and curve-fitting: A review of the literature. *Biochim. Biophys. Acta* **2009**, *1794*, 375–397.

(70) Uratani, Y.; Asakura, S.; Imahori, K. A circular dichroism study of Salmonella flagellin: Evidence for conformational change on polymerization. *J. Mol. Biol.* **1972**, *67*, 85–98.

(71) Prusiner, S. B. Novel proteinaceous infectious particles cause scrapie. *Science* **1982**, *216*, 136–144.

(72) Beaven, G. H.; Gratzer, W. B.; Davies, H. G. Formation and structure of gels and fibrils from glucagon. *Eur. J. Biochem.* **1969**, *11*, 37–42.

(73) Hofrichter, J.; Ross, P. D.; Eaton, W. A. Kinetics and mechanism of deoxyhemoglobin S gelation: A new approach to understanding sickle cell disease. *Proc. Natl. Acad. Sci. U.S.A.* **1974**, *71*, 4864–4868.

(74) Jarrett, J. T.; Lansbury, P. T., Jr. Seeding one-dimensional crystallization of amyloid: A pathogenic mechanism in Alzheimer's disease and scrapie. *Cell* **1993**, *73*, 1055–1058.

(75) Serio, T. R.; Cashikar, A. G.; Kowal, A. S.; Sawicki, G. J.; Moslehi, J. J.; Serpell, L.; Arnsdorf, M. F.; Lindquist, S. L. Nucleated conformational conversion and the replication of conformational information by a prion determinant. *Science* **2000**, *289*, 1317–1321.